JOURNAL OF OPTOELECTRONICS AND ADVANCED MATERIALS Vol. 10, No. 5, May 2008, p. 1159 - 1164

Eddy current analysis for ECT of a conductor with a conductive crack by Boundary Element Method

KAZUHISA ISHIBASHI
Department of Mechanical Engineering, Faculty of Engineering, Tokai University
2-28-4 Tomigaya, Shibuya-ku, Tokyo, 151-0063 Japan

We study how to solve eddy currents induced in a conductor with a conductive crack in order to apply to the eddy current testing (ECT). The eddy current is formulated by boundary integral equations whose unknowns are the surface electric and magnetic currents. When the skin depth is thick, computational error is increased in obtaining electromagnetic fields near the edge of the crack especially in the case of the conductive crack, and so we derive another integral equations by introducing a loop magnetic current on the crack surface. So as to check the validity of the proposed approach, we solve a typical ECT problem and compare the computed results with those by FEM.

(Received March 13, 2008; accepted May 5, 2008)

Keywords: Conductive crack, Eddy current testing, Loop magnetic current, Surface integral equation

1. Introduction

The finite element method (FEM) is widely employed for analyzing electromagnetic problems. Even if FEM is universal, it is not enough because adequacy of the computed results has to be checked in most of the cases, and experimental means used to be employed to check them. As computer technology has been developed, compatible numerical analyses with FEM have taken the place of them. As one of the compatible ones in eddy current analysis, we have the boundary element method (BEM), which has been widely used for analyzing open boundary electromagnetic problems [1].

Although the goal of the study on the eddy current testing (ECT) is to solve the inverse problem, a fast and accurate solution of the forward problem is regarded as a prerequisite for solving the inverse problem. If we employ the surface integral equations to solve ECT problems, we cannot get accurate solutions due to singular kernels at edges of the conductor. ECT is a type of nondestructive methods for detecting a crack in a conductor or on the surface of the conductor by applying an electromagnetic field with a frequency of thick skin depth and detecting affected fields by the crack. Some edges and corners of the crack are so close that it is difficult to get accurate solutions, moreover, as the width of the crack becomes narrower compared with its depth, the surface integral equations become ill conditioned and so it becomes more difficult.

Two kinds of BEM approaches for ECT analysis have been reported. One is a superposition model, in which the crack is replaced by a virtual source so that the current density at the crack becomes zero [2-5]. The other is a direct model, in which the electromagnetic fields on the interfaces are determined so that the boundary conditions are fulfilled [6-8].

By taking full advantage of integral representations of electromagnetic fields for a semi-infinite medium, the surface electric and magnetic currents are formulated with the help of the moment method [6]. In similar concept approaches, thanks to the dyadic Green's function, which satisfies the electromagnetic boundary conditions on the air-conductor surface of a half-space conductor or an infinite slab conductor, the virtual source is formulated by an integral equation [2-4]. These approaches cannot be applied to general ECT analyses due to restriction by the green's function. In another approach, the electric field perturbed due to the variation of the eddy current by the crack is represented by an integral equation, and then formulated by the weighted residual approach so as to impose Ohm's law [5]. It seems that this approach works on a condition that the crack is located so far from the end of the conductor that the original air-conductor boundary conditions may not be affected by the superposition. An effective approach by a direct model for a zero-gap crack has been reported [7] and this has been extended to apply to general eddy current problems [8]. In these approaches, the eddy current at a crack has been formulated by a line integral equation with a loop magnetic current as the unknown.

It is regarded as important to solve the inverse problem concerned with a conductive crack [9, 10].

In this paper, firstly, we formulate the eddy current induced in a conductor with a conductive crack by utilizing an ordinary technique given in [1] and point out computed error is increased as the width of the crack approaches zero. Next, on the basis of the formulation given in [7, 8], we derive a line integral equation to solve eddy currents induced in a conductor with a conductive crack, which is available even if the crack width approaches zero. Lastly, in order to check the validity of the proposed method, we solve a typical ECT problem and compare the computed results with those by FEM.

2. Formulation of eddy current

2.1 Integral representations of electromagnetic fields

The integral representations of electromagnetic fields are derived from Maxwell's equations by applying Green's theorem [11]. The magnetic and electric fields, $\boldsymbol{H}_{op}$ and $\boldsymbol{E}_{op}$, in space with a permeability μ_o and permittivity ε_o, and those, $\boldsymbol{H}_{ip}$ and $\boldsymbol{E}_{ip}$, in a conductor with a permeability μ_i and conductivity σ, are given as

$$\boldsymbol{H}_{op} = \boldsymbol{H}_{ep} + \int_S [\boldsymbol{J}_{so} \times \nabla G_o + H_{no} \nabla G_o] dS \tag{1}$$

$$\boldsymbol{E}_{op} = \boldsymbol{E}_{ep} - \int_S [j\omega\mu_o \boldsymbol{J}_{so} G_o + \boldsymbol{K}_{so} \times \nabla G_o + E_{no} \nabla G_o] dS \tag{2}$$

$$\boldsymbol{H}_{ip} = -\int_S [\sigma \boldsymbol{K}_{si} G_i + \boldsymbol{J}_{si} \times \nabla G_i + H_{ni} \nabla G_i] dS \tag{3}$$

$$\boldsymbol{E}_{ip} = \int_S [j\omega\mu_i \boldsymbol{J}_{\mathrm{si}} G_i + \boldsymbol{K}_{\mathrm{si}} \times \nabla G_i + E_{\mathrm{ni}} \nabla G_i] dS \tag{4}$$

where ω is the angular frequency, $\boldsymbol{H}_{\mathrm{ep}}$ and $\boldsymbol{E}_{\mathrm{ep}}$ are the exciting magnetic and electric fields at a observation point P_{o} produced by electromagnetic sources, respectively, S is the surface of the conductor, the subscript p is for denoting that the values are ones at P_{o} and $j=\sqrt{-1}$. Also, the electric and magnetic currents, $\boldsymbol{J}_{\mathrm{s}}$ and $\boldsymbol{K}_{\mathrm{s}}$ are defined as

$$\begin{aligned} \boldsymbol{J}_{\mathrm{so}} &= \boldsymbol{n} \times \boldsymbol{H}_{\mathrm{so}}, \quad \boldsymbol{J}_{\mathrm{si}} = \boldsymbol{n} \times \boldsymbol{H}_{\mathrm{si}}, \\ \boldsymbol{K}_{\mathrm{so}} &= -\boldsymbol{n} \times \boldsymbol{E}_{\mathrm{so}}, \quad \boldsymbol{K}_{\mathrm{si}} = -\boldsymbol{n} \times \boldsymbol{E}_{\mathrm{si}}, \end{aligned} \tag{5}$$

the normal components, H_{n}, E_{n}, of $\boldsymbol{H}_{\mathrm{s}}$ and $\boldsymbol{E}_{\mathrm{s}}$ are defined as

$$\begin{aligned} H_{\mathrm{no}} &= \boldsymbol{n} \cdot \boldsymbol{H}_{\mathrm{so}}, \quad H_{\mathrm{ni}} = \boldsymbol{n} \cdot \boldsymbol{H}_{\mathrm{si}}, \\ E_{\mathrm{no}} &= \boldsymbol{n} \cdot \boldsymbol{E}_{\mathrm{so}}, \quad E_{\mathrm{ni}} = \boldsymbol{n} \cdot \boldsymbol{E}_{\mathrm{si}} \end{aligned} \tag{6}$$

where $\boldsymbol{E}_{\mathrm{s}}$, $\boldsymbol{H}_{\mathrm{s}}$ are the electric and magnetic fields on the surface of the conductor with subscripts o and i denoting that the values are respectively of the outside and inside of the conductor, $\boldsymbol{n}$ is the unit normal directed from the inside to the outside of the conductor,

$$G_o = \frac{1}{4\pi r}, \qquad G_i = \frac{\exp(-k_i r)}{4\pi r}, \quad k_i = \sqrt{j\omega\mu_i\sigma} \tag{7}$$

with the distance r from a point on the surface to P_o.

From the continuity of the tangential components of the magnetic and electric fields, $\boldsymbol{J}_{\mathrm{s}}$ and $\boldsymbol{K}_{\mathrm{s}}$ must satisfy

$$\boldsymbol{J}_s = \boldsymbol{J}_{so} = \boldsymbol{J}_{si}, \quad \boldsymbol{K}_s = \boldsymbol{K}_{so} = \boldsymbol{K}_{si}. \tag{8}$$

From Maxwell's equation,

$$\begin{aligned} E_{no} &= -\nabla \cdot \boldsymbol{J}_s / (j\omega\varepsilon_o), \quad E_{ni} = -\nabla \cdot \boldsymbol{J}_s / \sigma \\ H_{no} &= -\nabla \cdot \boldsymbol{K}_s / (j\omega\mu_o), \quad H_{ni} = -\nabla \cdot \boldsymbol{K}_s / (j\omega\mu_i). \end{aligned} \tag{9}$$

2.2 Integral equations for solving $\mathbf{J}_s$ and $\mathbf{K}_s$

The electromagnetic fields have been given in (1)-(4). Here, we define the integral kernels as follows.

$$\Delta\boldsymbol{H}_o = \boldsymbol{J}_s \times \nabla G_o - \frac{\nabla \cdot \boldsymbol{K}_s}{j\omega\mu_o} \nabla G_o \tag{10}$$

$$\Delta\boldsymbol{H}_i = \sigma_i \boldsymbol{K}_s G_i + \boldsymbol{J}_s \times \nabla G_i - \frac{\nabla \cdot \boldsymbol{K}_s}{j\omega\mu_i} \nabla G_i \tag{11}$$

$$\Delta\boldsymbol{E}_i = j\omega\mu_i \boldsymbol{J}_s G_i + \boldsymbol{K}_s \times \nabla G_i - \frac{\nabla \cdot \boldsymbol{J}_s}{\sigma_i} \nabla G_i \tag{12}$$

It is available to employ (2) in the eddy current formulation, but it is not expected to get correct numerical solutions because E_{no} of the last term is numerically indeterminate as given in (9), and therefore (2) is omitted.

Fig. 1 shows a conductor with a conductive crack where S_c is a part of the conductor surface, S_g is the face-to-face surface of the crack, S_{gb} and S_{gt} are respectively the bottom and top surfaces of the crack, the subscripts c and g attached to the conductivity σ and relative permeability μ_r are respectively for denoting that the values are of the conductor and crack.

The formulation for $\boldsymbol{J}_s$ and $\boldsymbol{K}_s$ is as follows.

A. Choosing P_O on the surface S_c or S_{gt}, and taking the vector product of $\boldsymbol{n}_p$ and $\boldsymbol{H}_o$ in (1) and integrating $\boldsymbol{n}_p \times \boldsymbol{H}_o$ in the space side surface over S_c and S_{gt}, we get

$$\boldsymbol{J}_{sp}/2 + \boldsymbol{n}_p \times \left[\int_{S_c + S_{gt}} \Delta\boldsymbol{H}_o dS \right] = \boldsymbol{n}_{op} \times \boldsymbol{H}_{ep} \tag{13}$$

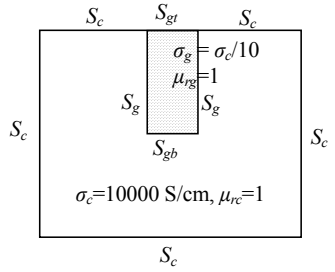

Fig.1. Conductor with a conductive crack.

B. Choosing P_O on the surface S_c, taking the vector product of $\boldsymbol{n}_p$ and $\boldsymbol{E}_i$ in (4) and integrating $\boldsymbol{n}_p \times \boldsymbol{E}_i$ in the conductor side surface over S_c, S_g and S_{gb}, we get

$$\boldsymbol{K}_{sp}/2 - \boldsymbol{n}_p \times \left[\int_{S_c + S_g + S_{gb}} \Delta\boldsymbol{E}_c dS \right] = 0 \tag{14}$$

where the subscript c denotes the value in the conductor.

C. Choosing P_O on the surface S_g or S_{gb}, taking the vector product of $\boldsymbol{n}_p$ and $\boldsymbol{H}_i$ in (3) and integrating $\boldsymbol{n}_p \times \boldsymbol{H}_i$ in the conductor side surface over S_c, S_g and S_{gb}, we get one integral equation. Choosing P_O on the same position, taking the same procedure and integrating $\boldsymbol{n}_p \times \boldsymbol{H}_i$ in the crack side over S_g, S_{gb} and S_{gt}, we get another integral equation. Subtracting one from the other, we get

$$\boldsymbol{J}_{sp} + \boldsymbol{n}_p \times \left[\int_{S_c + S_g + S_{gb}} \Delta\boldsymbol{H}_c dS - \int_{S_g + S_{gb} + S_{gt}} \Delta\boldsymbol{H}_g dS \right] = 0 \tag{15}$$

where the subscript g denotes the value in the crack..

D. Choosing P_o on S_{gt}, taking the vector product of $\boldsymbol{n}_p$ and $\boldsymbol{E}_i$ in (4) and integrating $\boldsymbol{n}_p \times \boldsymbol{E}_i$ in the crack side over S_g, S_{gb} and S_{gt}, we get

$$\boldsymbol{K}_{sp}/2 - \boldsymbol{n}_p \times \int_{S_g+S_{gb}+S_{gt}} \Delta \boldsymbol{E}_g dS = 0 \tag{16}$$

E. Choosing P_o on the surface S_g or S_{gb}, taking the vector product of $\boldsymbol{n}_p$ and $\boldsymbol{E}_i$ in (4) and integrating $\boldsymbol{n}_p \times \boldsymbol{E}_i$ in the conductor side over S_c, S_g and S_{gb}, we get one integral equation. Choosing P_o on the same point, taking the same procedure and integrating $\boldsymbol{n}_p \times \boldsymbol{E}_i$ in the crack side over S_g, S_{gb} and S_{gt}, we get another integral equation. Subtracting one from the other, we get

$$\boldsymbol{K}_{sp} - \boldsymbol{n}_p \times \left[\int_{S_c+S_g+S_{gb}} \Delta \boldsymbol{E}_c dS - \int_{S_g+S_{gb}+S_{gt}} \Delta \boldsymbol{E}_g dS \right] = 0 \tag{17}$$

We have been derived equations (13-17) to determine the unknowns $\boldsymbol{J}_s$ and $\boldsymbol{K}_s$. As the crack width approaches zero, the equations for determining $\boldsymbol{J}_s$ and $\boldsymbol{K}_s$ on the face-to-face surface tend to be ill conditioned because both the equations approach the same. On the conductor side, $\boldsymbol{K}_s$ becomes ill conditioned, and on the crack side, $\boldsymbol{J}_s$ becomes ill conditioned. So as to get reasonable answers, if we choose the integral equation derived from the magnetic field on the conductor side, then we have to choose the one derived from the electric field on the crack side, and vise versa. On these reasons, we can't expect accurate solutions if the crack width is thin enough compared with the crack depth.

2.3 Introduction of loop magnetic current K_l for K_s

Accuracy of the solution by the integral equations (13)-(17) tends to be worse as the crack width approaches zero. We shall introduce a loop magnetic current so as to get accurate solutions even if the crack width becomes almost zero.

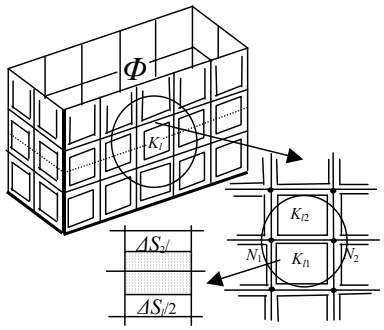

Fig. 2. Lumped loop magnetic current for analyzing eddy current at the crack

From Faraday's laws of electromagnetic induction that the time rate of decrease of magnetic flux Φ through the crack equals the line integral of the electric field along the closed path C shown by the dotted line in Fig. 2, we get

$$\oint_C (\boldsymbol{n}_g \times \boldsymbol{K}_s) \cdot d\boldsymbol{C} = -j\omega\mu \int_{S_C} \boldsymbol{H} \cdot d\boldsymbol{S}_C \tag{18}$$

where S_C is the area enclosed by C, $\boldsymbol{n}_g$ is the unit normal to the crack surface, μ is the permeability and $\boldsymbol{H}$ is the magnetic field given by (1) or (3).

As S_C =0 when the crack gap g_w is zero, we get from (18)

$$\oint_C (\boldsymbol{n}_g \times \boldsymbol{K}_s) \cdot d\boldsymbol{C} = 0 \tag{19}$$

Focusing on (19), we shall introduce a lumped loop magnetic current K_l as shown in Fig. 2, instead of $\boldsymbol{K}_s$, so as to satisfy (19) automatically. The loop magnetic current K_l circulates along the periphery of the surface element as shown in Fig. 2. At the crack aperture, K_l is not closed but open because Φ is zero on the condition that the circulating path is always on the conductor surface. Therefore, if the path goes into space at the aperture, (19) is not satisfied even if g_w = 0. In other words, K_l ensures that the line integral of electric field along the closed path C is zero.

The rotational surface magnetic current $\boldsymbol{K}_s$ corresponding to K_l is obtained as follows. In Fig. 2, two lumped loop magnetic current, K_{l1} and K_{l2}, flow at the edge from the node N_1 to N_2. These lumped currents flow originally on the shaded surfaces, $\Delta S_1/2$ and $\Delta S_2/2$, shown in the same figure. From these concepts, we define the magnitude of $\boldsymbol{K}_s$ at the element edge as

$$K_s = \frac{2(w_2 K_{l2} - w_1 K_{l1})\Delta L}{\Delta S_1 + \Delta S_2} \tag{20}$$

where ΔS_1 and ΔS_2 are respectively the surface of the element of which periphery K_{l1} and K_{l2} flow, ΔL is the length from N_1 to N_2 and w_1 and w_2 are the weight functions defined as

$$w_1 = \frac{\Delta S_2}{\Delta S_1 + \Delta S_2}, \qquad w_2 = \frac{\Delta S_1}{\Delta S_1 + \Delta S_2} \tag{21}$$

and the direction of $\boldsymbol{K}_s$ is from the node N_1 to N_2.

Even at the crack edge, $\boldsymbol{K}_s$ are defined in the same way as that of the smooth surface. At the aperture edge, as the induced current does not flow into space, the electric field perpendicular to the aperture edge is zero. And so,

$$K_{se} = 0 \tag{22}$$

where K_{se} is the component of $\boldsymbol{K}_s$ parallel to the aperture edge.

2.4 Integral equations for solving K_l

The loop magnetic current K_l is determined by a line integral equation derived as follows.

Choosing P_o on the surface S_g or S_{gb}, taking the scalar product of $\boldsymbol{n}_p$ and $\boldsymbol{E}_i$ in (4) to obtain the current density and integrating $\boldsymbol{n}_p \cdot \boldsymbol{E}_i$ in the conductor side over S_c, S_g and S_{gb}, we get one integral equation. Taking the same

procedure and integrating $\boldsymbol{n}_p \cdot \boldsymbol{E}_i$ in the crack side over S_g, S_{gb} and S_{gt}, we get another integral equation. Enforcing the current density continuity condition, we get

$$\boldsymbol{n}_p \cdot \left[\int_{S_c+S_g+\Delta S_{gb}} \Delta \boldsymbol{E}_c dS + \left(\sigma_g/\sigma_c\right) \int_{S_g+S_{gb}+S_{gt}} \Delta \boldsymbol{E}_g dS \right] = 0 \qquad (23)$$

The equation (23) is employed instead of (17). In this case, the integral kernels of (13)-(16) and (23) are not exactly the same as those given in (10)-(12). The surface magnetic current $\boldsymbol{K}_s$ on the crack surface is changed to K_l and surface integral to line integral.

If the crack width between the face-to-face surfaces approaches zero, we can utilize the following relations [7]. On the basis that $\boldsymbol{n}_1$=-$\boldsymbol{n}_2$, $\boldsymbol{H}_{s1}$=$\boldsymbol{H}_{s2}$ and $\boldsymbol{E}_{s1}$=-$\boldsymbol{E}_{s2}$, we get

$$\boldsymbol{J}_{s1} = -\boldsymbol{J}_{s2}, \qquad \boldsymbol{K}_{s1} = \boldsymbol{K}_{s2} \qquad (24)$$

where the subscripts 1 denotes that the value is on the one side of the face-to-face surfaces and 2 denotes the one on the other side.

If the crack gap is not regarded as zero, we can analyze the electromagnetic fields by employing the approach given in [8], where the magnetic flux through the crack is taken into consideration.

2.4 Integral formulas of electromagnetic fields in conductor

Here, we shall derive integral formulas to improve the accuracy of computed results. On the face-to-face surface, $\boldsymbol{J}_s$ and $\boldsymbol{K}_s$ on one side are determined dominantly by those on the other side, and so it is helpful to get integral formulas for evaluating analytically the electromagnetic fields without the help of numerical calculation.

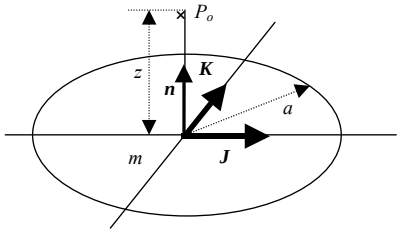

Fig. 3. Electromagnetic fields in conductor produced by $\boldsymbol{J}_s$, $\boldsymbol{K}_s$ and H_n.

If the electromagnetic field on a flat surface is uniform, the electromagnetic field in conductor at P_o above the center of the disk face shown in Fig.3 can be evaluated analytically. The integral terms contained in (3) are given as follows.

$$\int [\boldsymbol{K} G_i] dS = \frac{\boldsymbol{K}}{4\pi} \int \frac{e^{-\gamma_i \sqrt{r^2+z^2}}}{\sqrt{r^2+z^2}} 2\pi r dr = \frac{-\boldsymbol{K}}{2\gamma_1} e^{-\gamma_i \sqrt{r^2+z^2}} \qquad (25)$$

$$\int [\boldsymbol{J} \times \nabla G_i] dS = \frac{\boldsymbol{J} \times \boldsymbol{n}}{4\pi} \int \left[\frac{\gamma_i z}{\sqrt{r^2+z^2}} e^{-\gamma_i \sqrt{r^2+z^2}} + \frac{1}{\left(r^2+z^2\right)^{\frac{3}{2}}} e^{-\gamma_i \sqrt{r^2+z^2}} \right] 2\pi r dr = \frac{-\boldsymbol{J} \times \boldsymbol{n}}{2} \frac{z}{\sqrt{r^2+z^2}} e^{-\gamma_i \sqrt{r^2+z^2}} \qquad (26)$$

$$\int [m \nabla G_i] dS = \frac{-m}{2} \boldsymbol{n} \frac{z}{\sqrt{r^2+z^2}} e^{-\gamma_i \sqrt{r^2+z^2}} \qquad (27)$$

where $\boldsymbol{n}$ is a unit vector toward the observation point P_o from the disk face S, z is distance from S to P_o and r is radius. The integral terms in (4) are given in the same way.

3. Eddy current analysis

3.1 Check of eddy current formulation

In order to test validity of the proposed method, we solve a 2D eddy current problem shown in Fig.1. The width and height of the conductor are 4 and 1.25 mm. The width and depth of the crack at the middle of the upper conductor surface are 0.005 and 0.75 mm. The conductivity of the conductor: σ=1000 S/mm, the relative permeability: μ_r =1, the conductivity of the conductive crack is supposed to be as σ_g=σ_c/10 and the relative permeability: μ_{rg} =1. The conductor is placed parallel to a uniform magnetic field (H_e=1 A/cm, f=300 kHz).

In solving the integral equations, we employ the constant surface element for $\boldsymbol{J}_s$ and $\boldsymbol{K}_s$. Here, we shall describe how to evaluate the surface magnetic charge m_s and electric charge q_s contained in (10-12). As given these equations, these charges are obtained by the surface divergence of $\boldsymbol{J}_s$ and $\boldsymbol{K}_s$. When these values are constant on the surface element, the surface divergence is zero within the element and it appears only at edges of the element. As the value at the edge is given by δ function, the surface integral is evaluated by line integral.

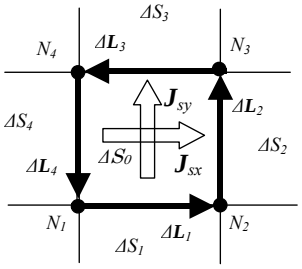

Fig. 4. Surface electric charge produced by J_s.

The line electric charge Q_i is given as follows.

$$Q_i = q_{si} dw = \left(\boldsymbol{J}_s \times \Delta \boldsymbol{L}_i\right) \cdot \boldsymbol{n}_s, \; i=1, 2, 3 \text{ and } 4 \qquad (28)$$

where subscripts i denotes that the value corresponds to the surface element edge shown in Fig. 4, dw is the width of the edge, $\Delta \boldsymbol{L}_i$ is the distance from N_i to N_{i+1}, $\boldsymbol{n}_s$ is the unit normal of the element and $\boldsymbol{J}_s$= $\boldsymbol{J}_{sx}$ + $\boldsymbol{J}_{sy}$. The line magnetic charge M_i is given in the same way.

Next, we shall obtain the surface electric charge q_s, which is necessary when the eddy current is formulated by $\boldsymbol{J}_s$, $\boldsymbol{K}_s$ and K_l. The line electric charge Q, which appears at each

edge of the surface element, has been obtained as in (28). The line charge is originally on the adjoining surfaces in the similar way as the lumped magnetic current shown in Fig. 2, and q_s is given by adding an average value of the line charges.

$$q_S = \sum_{i=1}^{4} \frac{Q_{0i}}{\Delta S_0 + \Delta S_i} \tag{29}$$

where ΔS_0 and ΔS_i are respectively the center and adjoining surface of the element shown in Fig. 4, Q_{0i} is the line charge at i-th edge defined as

$$Q_{0i} = \left(w_0 \boldsymbol{J}_{s0} - w_i \boldsymbol{J}_{si}\right) \cdot \boldsymbol{n}_s \tag{30}$$

with the subscript 0 and i denoting that the values are respectively of the center and adjoining element, and

$$w_0 = \Delta S_i / \left(\Delta S_0 + \Delta S_i\right), \qquad w_i = \Delta S_0 / \left(\Delta S_0 + \Delta S_i\right).$$

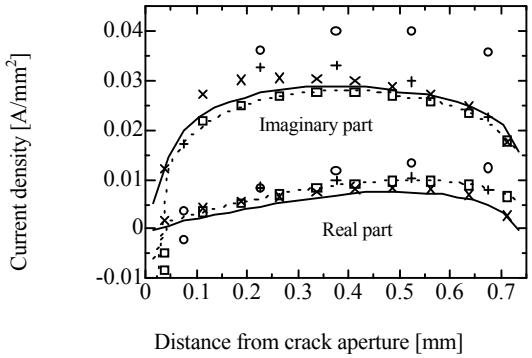

Fig. 5. Computed results of current density on crack surface.

We have derived two types of the integral equations. One type is composed of the integral equations with $\boldsymbol{J}_s$ and $\boldsymbol{K}_s$ as unknowns, the other with $\boldsymbol{J}_s$, $\boldsymbol{K}_s$ and K_l. Here, we call the former '$\boldsymbol{J}_s$-$\boldsymbol{K}_s$ approach', and the latter '$\boldsymbol{J}_s$-$\boldsymbol{K}_s$-K_l approach'. We shall evaluate these integral equations.

The computed results of the parallel components of the current density to the crack surface are shown in Fig.5. The dotted and solid lines are the computed results by $\boldsymbol{J}_s$-$\boldsymbol{K}_s$ and $\boldsymbol{J}_s$-$\boldsymbol{K}_s$-K_l approaches, respectively. These are almost the same because the surface element size is fine enough. In the case of rough meshes, the results at the center of the element are shown by +, ×, □ and ○. It is noticed that $\boldsymbol{J}_s$-$\boldsymbol{K}_s$-K_l approach gives rather accurate results as shown by + and ×, but the accuracy by $\boldsymbol{J}_s$-$\boldsymbol{K}_s$ approach becomes poor as shown by □ and ○.

3.2 Eddy current analysis of a conductor with a crack

Next, we solve an ECT model shown in Fig. 6. The model is a modified model of the benchmark model [12]. There is a crack on top surface of a metal plate ($4 \times 4 \times 1.25$ mm). The crack width is 3 mm, depth is 0.75 mm and the width is 0.1 mm. The gap between the lower surface of the coil and the upper surface of the plate is 0.5 mm. A doughnut-type exciting coil is placed above the center of the crack. Inner and outer diameters of the coil are 1.2 and 3.2 mm, the height of the coil is 0.8 mm. The current of the coil is 1 AT and its frequency is 300 kHz. Conductivity and relative permeability of the plate are σ=1000 S/mm and μ_r=1. Those of the conductive crack are σ_g=100 S/mm and μ_r=1.

So as to show computed results, we shall set x-y-z axes on the lower plate surface. The origin of the coordinates is at its center. The x-axis is along the crack and the z-axis is perpendicular to the upper plate surface. Fig. 7 and 8 show typical computed results of the tangential components of the current density along on the broken lines shown in Fig. 6.

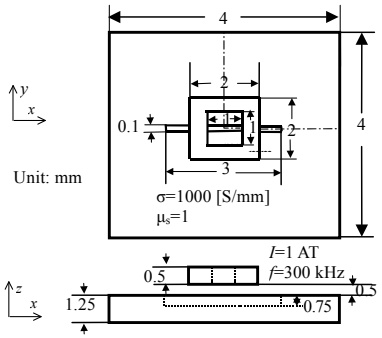

Fig. 6. Analysis model.

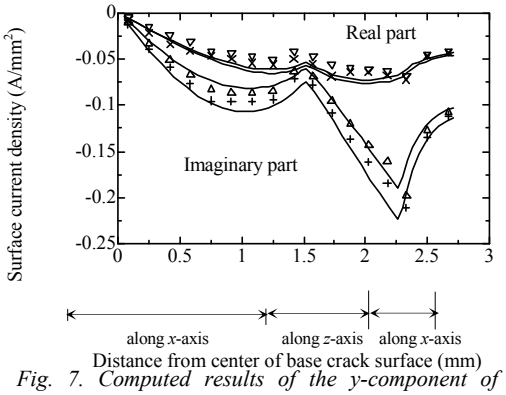

Fig. 7. Computed results of the y-component of the current density on the base crack surface along x-axis at y=0, z=0.5 mm, that on the lateral crack surface along z-axis at x = 1.5, y=0 mm, and that on the upper plate surface along x-axis at y=0, z=1.25 mm

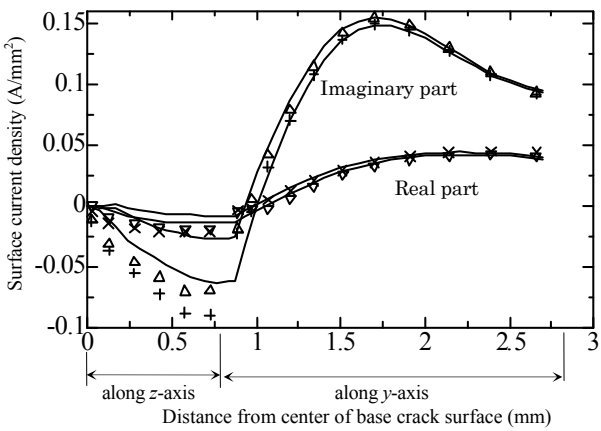

Fig. 8. Computed results of the x-component of the current density on the lateral crack surface along z-axis at x=0, y = 0 mm, and that on the upper plate surface along y-axis at x=0, z=1.25 mm.

As $\boldsymbol{J}_s$-$\boldsymbol{K}_s$ approach does not give reasonable results, here, the computed results only by $\boldsymbol{J}_s$-$\boldsymbol{K}_s$-K_l approach are shown. The solid lines show the results by FEM, + and × show those in case of non-conductive crack, and Δ and ∇ in case of conductive crack by the proposed method. There are some discrepancies between them. It depends mainly on the way to estimate $\boldsymbol{K}_s$ from K_l according to (20). As the crack width becomes narrow, the estimation of $\boldsymbol{K}_s$ becomes critical. However, this is not essential in ECT analysis because the computed value of K_l is directly employed for ECT analysis without estimating $\boldsymbol{K}_s$ from K_l. Therefore, it is not the matter whether we estimate $\boldsymbol{K}_s$ correctly or not in ECT analysis.

4. Conclusions

We have studied an approach to analyze the eddy current in a conductor with a conductive crack.

Firstly, thanks to the common formulation by BEM, we have derived a set of the integral equations with the surface electric and magnetic currents, $\boldsymbol{J}_s$ and $\boldsymbol{K}_s$ as unknowns. However, the integral equations do not give accurate computed values as the crack width become narrow.

Next, introducing the rotational magnetic current $\boldsymbol{K}_s$, obtaining the normal component of electric field on the crack surface, and enforcing the continuity boundary condition of the current density, we have derived another set of the integral equations, which are available even in case of zero crack width. The integral equations have been discretized with the constant elements for $\boldsymbol{J}_s$, $\boldsymbol{K}_s$ and the loop magnetic current K_l.

Finally, in order to check the validity of the proposed method, we have solved an ECT problem and compared computed results with those by FEM.

From these studies, it is confirmed that the proposed method becomes an effective tool for ECT analysis.

References

[1] Johnson J. H. Wang, Generalized Moment Method in Electromagnetics, John Wiley & Sons, 1991.
[2] Y. Yoshida, J. R. Bowler, IEEE Trans. Magn. **36**, 461 (2000).
[3] O. Michelsson, F. H. Uhlmann, IEEE Trans. Magn. **36**, 756 (2000).
[4] D. Chen, K. R. Shao, J. D. Lavers, IEEE Trans. Magn. **38**, 2355 (2002).
[5] R. Albanese, G. Rubinacci, F. Villone, Journal of Computational Physics **152**, 736 (1999).
[6] X. Lou, P. K. Kadaba, J. Li, IEEE Trans. Magn. **29**, 2244 (1993).
[7] K. Ishibashi, IEEE Trans. Magn., **41**, 1400 (2005).
[8] K. Ishibashi, IEEE Trans. Magn., **42**, 787 (2006).
[9] F. Vollone, IEEE Trans. Magn., **36**, 1706 (2006).
[10] Z. Chen, M. Rebican, N. Yusa, K. Miya, IEEE Trans. Magn. **42**, 683 (2006).
[11] J. A. Stratton, Electromagnetic Theory, McGRAW-HILL, (1941) 464-466
[12] T. Takagi, M. Hashimoto, H. Fukutomi, M. Kurokawa, K. Miya, H. Tsuboi, J. Tani, T. Serizawa, Y. Harada, E. Okano, R. Murakami, International Journal of Applied Electromagnetics and Mechanics, **5,** 149 (1994).

*Corresponding author: isibasi@keyaki.cc.u-tokai.ac.jp